

Dirac–Fock calculations of forbidden transitions within the $3p^k$ and $3d^k$ ground configurations of highly charged tungsten ions (W^{47+} – W^{61+})

This article has been downloaded from IOPscience. Please scroll down to see the full text article.

2011 J. Phys. B: At. Mol. Opt. Phys. 44 195007

(<http://iopscience.iop.org/0953-4075/44/19/195007>)

View the [table of contents for this issue](#), or go to the [journal homepage](#) for more

Download details:

IP Address: 193.190.193.1

The article was downloaded on 13/09/2011 at 15:47

Please note that [terms and conditions apply](#).

Dirac–Fock calculations of forbidden transitions within the $3p^k$ and $3d^k$ ground configurations of highly charged tungsten ions (W^{47+} – W^{61+})

Pascal Quinet

Astrophysique et Spectroscopie, Université de Mons—UMONS, B-7000 Mons, Belgium
IPNAS, Université de Liège, B15 Sart Tilman, B-4000 Liège, Belgium

E-mail: quinet@umons.ac.be

Received 17 June 2011, in final form 3 August 2011

Published 13 September 2011

Online at stacks.iop.org/JPhysB/44/195007

Abstract

Wavelengths and transition probabilities have been computed for forbidden lines within the $3p^k$ and $3d^k$ ground configurations of tungsten ions from W^{47+} to W^{61+} . The fully relativistic multiconfiguration Dirac–Fock method was used for the calculations. They take into account the correlations within the $n = 3$ complex, some $n = 3 \rightarrow n' = 4$ single excitations and quantum electrodynamics effects. The present results are compared to and agree very well with experimental wavelengths and theoretical transition probabilities previously published for a few lines.

1. Introduction

It is well known that spectroscopic parameters of tungsten ions are essential for exploring the physical conditions in tokamak plasmas such as ITER in which tungsten is currently considered to be a primary candidate for the plasma-facing material in the divertor region (see e.g. Hawryluk *et al* 2009). In this context, forbidden lines play an important role in plasma diagnostics because the corresponding radiation intensities are often very sensitive to electron temperature and density. Therefore, wavelengths and transition rates for such forbidden lines in various ionization stages of tungsten must be determined with high confidence from theoretical calculations or experimental measurements.

Up to now, about 120 forbidden lines in tungsten ions, from W^{28+} to W^{57+} , were observed experimentally in tokamak or electron-beam ion trap (EBIT) spectra in ultraviolet (Utter *et al* 2000, Porto *et al* 2000), vacuum ultraviolet (Radtke *et al* 2007), extreme ultraviolet (Pütterich *et al* 2005, Ralchenko *et al* 2007, 2008, 2011a) and x-ray (Tragin *et al* 1988, Neu *et al* 1997, 2001, Ralchenko *et al* 2006, Clementson *et al* 2010) ranges. More particularly, an EBIT source was recently used by Ralchenko *et al* (2011a) to measure extreme ultraviolet spectra between 10 and 25 nm from

highly charged ions of tungsten with an open 3d shell. These authors found that almost all strong lines were due to the forbidden magnetic dipole (M1) transitions within the $3d^k$ ground configurations. In this latter work, a total of 37 previously unknown spectral lines were identified using detailed collisional-radiative modelling of the EBIT spectra.

On the theoretical side, different investigations of forbidden transitions in tungsten ions were published so far. In the 1980s, extensive multiconfiguration Dirac–Fock (MCDF) calculations of radiative decays along Cl, S, P, Si and Al isoelectronic sequences were achieved. In these works, some forbidden lines in the $3p^k$ configurations were listed for W^{57+} (Huang *et al* 1983), W^{58+} (Saloman and Kim 1989), W^{59+} (Huang 1984), W^{60+} (Huang 1985) and W^{61+} (Huang 1986). Feldman *et al* (1991, 2001) and Doron and Feldman (2001) performed a systematic study of density-sensitive magnetic dipole lines in Ti-like ions including W^{53+} . Relativistic quantum defect orbital (RQDO) calculations of transition rates for electric quadrupole and magnetic dipole lines for ions along the potassium and aluminium isoelectronic sequences, including W^{55+} and W^{61+} , were carried out by Charro *et al* (2002, 2003), respectively. Atomic structure and radiative properties of forbidden transitions in Yb-like, Ag-like, Zn-like, Ca-like, Al-like, Mg-like, B-like and Be-like

Table 2. Forbidden transitions within the $3p^k$ and $3d^k$ ground configurations of tungsten ions. Only transitions with A -values greater than 10^6 s^{-1} are given except for a few experimentally observed lines. $X(Y)$ stands for $X \times 10^Y$.

Ion	Lower level ^a	Upper level ^a	$\lambda_{\text{exp}}^{\text{b}}$ (nm)	$\lambda_{\text{MCDF}}^{\text{c}}$ (nm)	Type	$A_{\text{MCDF}}^{\text{c}}$ (s^{-1})	A_{prev} (s^{-1})
W^{47+}	$3d^9[1]_{5/2}$	$3d^9[2]_{3/2}$	18.567	18.671	M1	2.46(6)	2.47(6) ^d
W^{48+}	$3d^8[6]_1$	$3d^8[9]_0$		15.174	M1	7.43(6)	
	$3d^8[1]_4$	$3d^8[7]_4$	15.511	15.503	M1	1.01(6)	1.01(6) ^d
	$3d^8[4]_3$	$3d^8[8]_2$		17.229	M1	4.14(6)	
	$3d^8[2]_2$	$3d^8[6]_1$	17.502	17.548	M1	1.70(6)	1.71(6) ^d
	$3d^8[2]_2$	$3d^8[5]_2$	18.878	18.978	M1	1.93(6)	1.93(6) ^d
	$3d^8[1]_4$	$3d^8[4]_3$	18.988	19.114	M1	3.20(6)	3.22(6) ^d
	$3d^8[5]_2$	$3d^8[8]_2$		19.847	M1	1.17(6)	
W^{49+}	$3d^7[7]_{5/2}$	$3d^7[18]_{5/2}$		12.721	M1	1.49(6)	
	$3d^7[3]_{5/2}$	$3d^7[12]_{3/2}$		13.660	M1	1.01(6)	
	$3d^7[1]_{9/2}$	$3d^7[10]_{7/2}$	14.166	14.156	M1	1.72(5)	1.76(5) ^d
	$3d^7[4]_{7/2}$	$3d^7[17]_{7/2}$		14.617	M1	1.13(6)	
	$3d^7[11]_{5/2}$	$3d^7[18]_{5/2}$		15.025	M1	1.66(6)	
	$3d^7[1]_{9/2}$	$3d^7[9]_{11/2}$	15.368	15.343	M1	1.89(5)	1.89(5) ^d
	$3d^7[13]_{5/2}$	$3d^7[19]_{3/2}$		15.764	M1	6.20(6)	
	$3d^7[5]_{9/2}$	$3d^7[17]_{7/2}$		15.945	M1	1.56(6)	
	$3d^7[5]_{9/2}$	$3d^7[16]_{9/2}$		16.619	M1	2.18(6)	
	$3d^7[14]_{3/2}$	$3d^7[19]_{3/2}$		16.631	M1	3.13(6)	
	$3d^7[4]_{7/2}$	$3d^7[13]_{5/2}$		17.069	M1	6.06(6)	
	$3d^7[6]_{3/2}$	$3d^7[15]_{1/2}$		17.143	M1	1.06(6)	
	$3d^7[1]_{9/2}$	$3d^7[5]_{9/2}$	17.106	17.149	M1	2.24(6)	2.23(6) ^d
	$3d^7[8]_{1/2}$	$3d^7[15]_{1/2}$		18.024	M1	3.41(6)	
	$3d^7[3]_{5/2}$	$3d^7[10]_{7/2}$	18.276	18.258	M1	2.82(5)	2.72(5) ^d
	$3d^7[6]_{3/2}$	$3d^7[14]_{3/2}$		18.568	M1	2.86(6)	
	$3d^7[9]_{11/2}$	$3d^7[16]_{9/2}$		18.759	M1	1.29(6)	
	$3d^7[2]_{3/2}$	$3d^7[8]_{1/2}$	18.670	18.764	M1	2.56(6)	2.56(6) ^d
	$3d^7[1]_{9/2}$	$3d^7[4]_{7/2}$	18.880	19.006	M1	3.55(6)	3.57(6) ^d
	$3d^7[2]_{3/2}$	$3d^7[7]_{5/2}$	19.047	19.130	M1	1.03(6)	1.03(6) ^d
	$3d^7[7]_{5/2}$	$3d^7[14]_{3/2}$		19.223	M1	2.78(6)	
	$3d^7[2]_{3/2}$	$3d^7[6]_{3/2}$		19.825	M1	1.59(6)	
	$3d^7[3]_{5/2}$	$3d^7[6]_{3/2}$		22.331	M1	1.71(6)	
W^{50+}	$3d^6[12]_1$	$3d^6[29]_0$		11.165	M1	3.96(6)	
	$3d^6[1]_4$	$3d^6[15]_3$	12.779	12.739	M1	3.95(5)	4.05(5) ^d
	$3d^6[1]_4$	$3d^6[14]_4$	13.137	13.114	M1	3.52(4)	3.68(4) ^d
	$3d^6[16]_2$	$3d^6[32]_2$		13.225	M1	1.04(6)	
	$3d^6[2]_2$	$3d^6[15]_3$	13.886	13.843	M1	4.90(5)	4.92(5) ^d
	$3d^6[2]_2$	$3d^6[13]_2$	14.193	14.184	M1	3.14(5)	3.20(5) ^d
	$3d^6[19]_3$	$3d^6[33]_3$		14.373	M1	2.73(6)	
	$3d^6[19]_3$	$3d^6[32]_2$		14.767	M1	2.92(6)	
	$3d^6[6]_1$	$3d^6[23]_1$		14.838	M1	1.68(6)	
	$3d^6[30]_1$	$3d^6[34]_0$		15.235	M1	1.52(7)	
	$3d^6[18]_4$	$3d^6[31]_4$		15.264	M1	4.25(6)	
	$3d^6[1]_4$	$3d^6[10]_3$	15.363	15.370	M1	1.01(6)	1.01(6) ^d
	$3d^6[7]_5$	$3d^6[24]_4$		15.386	M1	1.92(6)	
	$3d^6[4]_3$	$3d^6[19]_3$		15.888	M1	2.34(6)	
	$3d^6[20]_5$	$3d^6[31]_4$		16.139	M1	2.59(6)	
	$3d^6[5]_4$	$3d^6[19]_3$		16.220	M1	1.91(6)	
	$3d^6[14]_4$	$3d^6[27]_4$		16.277	M1	1.10(6)	
	$3d^6[9]_2$	$3d^6[25]_2$		16.503	M1	1.57(6)	
	$3d^6[16]_2$	$3d^6[30]_1$		16.606	M1	9.53(6)	
	$3d^6[23]_1$	$3d^6[32]_2$		16.837	M1	2.12(6)	
	$3d^6[15]_3$	$3d^6[27]_4$		16.894	M1	1.40(6)	
	$3d^6[5]_4$	$3d^6[18]_4$		16.983	M1	4.65(6)	
	$3d^6[8]_6$	$3d^6[21]_6$		17.061	M1	1.39(6)	
	$3d^6[1]_4$	$3d^6[7]_5$	17.133	17.118	M1	6.57(5)	6.57(5) ^d
	$3d^6[17]_0$	$3d^6[30]_1$		17.296	M1	2.40(6)	
	$3d^6[2]_2$	$3d^6[9]_2$		17.376	M1	2.02(6)	
	$3d^6[13]_2$	$3d^6[26]_2$		17.565	M1	1.74(6)	
	$3d^6[25]_2$	$3d^6[32]_2$		17.615	M1	1.29(6)	
	$3d^6[22]_3$	$3d^6[31]_4$		17.698	M1	1.23(6)	

Table 2. (Continued.)

Ion	Lower level ^a	Upper level ^a	$\lambda_{\text{exp}}^{\text{b}}$ (nm)	$\lambda_{\text{MCDF}}^{\text{c}}$ (nm)	Type	$A_{\text{MCDF}}^{\text{c}}$ (s ⁻¹)	A_{prev} (s ⁻¹)
W ⁵¹⁺	3d ⁶ [3]_0	3d ⁶ [12]_1	17.826	17.750	M1	1.32(6)	1.32(6) ^d
	3d ⁶ [8]_6	3d ⁶ [20]_5		17.920	M1	1.86(6)	
	3d ⁶ [15]_3	3d ⁶ [26]_2		18.119	M1	1.56(6)	
	3d ⁶ [4]_3	3d ⁶ [16]_2		18.168	M1	5.46(6)	
	3d ⁶ [10]_3	3d ⁶ [22]_3		18.304	M1	1.54(6)	
	3d ⁶ [6]_1	3d ⁶ [17]_0		18.666	M1	7.92(6)	
	3d ⁶ [1]_4	3d ⁶ [5]_4	19.239	19.303	M1	3.02(6)	3.02(6) ^d
	3d ⁶ [6]_1	3d ⁶ [16]_2		19.542	M1	1.63(6)	
	3d ⁶ [1]_4	3d ⁶ [4]_3	19.684	19.796	M1	2.56(6)	2.56(6) ^d
	3d ⁶ [26]_2	3d ⁶ [33]_3		20.267	M1	1.21(6)	
	3d ⁶ [2]_2	3d ⁶ [6]_1		20.778	M1	3.29(6)	
	3d ⁵ [21]_5/2	3d ⁵ [36]_3/2		12.350	M1	3.25(6)	
	3d ⁵ [16]_3/2	3d ⁵ [35]_1/2		12.930	M1	1.26(6)	
	3d ⁵ [12]_7/2	3d ⁵ [33]_5/2		13.391	M1	1.53(6)	
	3d ⁵ [4]_3/2	3d ⁵ [23]_1/2		13.698	M1	2.08(6)	
	3d ⁵ [10]_3/2	3d ⁵ [27]_5/2		14.046	M1	1.01(6)	
	3d ⁵ [12]_7/2	3d ⁵ [32]_9/2		14.087	M1	1.04(6)	
	3d ⁵ [28]_5/2	3d ⁵ [37]_5/2		14.271	M1	6.42(6)	
	3d ⁵ [2]_5/2	3d ⁵ [16]_3/2		14.399	M1	1.97(6)	
	3d ⁵ [9]_7/2	3d ⁵ [25]_9/2		14.431	M1	1.09(6)	
	3d ⁵ [1]_5/2	3d ⁵ [9]_7/2	14.531	14.475	M1	1.22(5)	1.21(5) ^d
	3d ⁵ [3]_7/2	3d ⁵ [21]_5/2		14.502	M1	1.53(6)	
	3d ⁵ [18]_5/2	3d ⁵ [33]_5/2		14.963	M1	1.69(6)	
	3d ⁵ [13]_11/2	3d ⁵ [31]_11/2		15.524	M1	3.43(6)	
	3d ⁵ [12]_7/2	3d ⁵ [29]_7/2		15.742	M1	2.12(6)	
	3d ⁵ [11]_5/2	3d ⁵ [28]_5/2		15.778	M1	8.27(6)	
	3d ⁵ [8]_1/2	3d ⁵ [23]_1/2		15.899	M1	1.51(6)	
	3d ⁵ [14]_9/2	3d ⁵ [31]_11/2		15.913	M1	1.03(6)	
	3d ⁵ [23]_1/2	3d ⁵ [35]_1/2		15.944	M1	2.61(6)	
	3d ⁵ [29]_7/2	3d ⁵ [37]_5/2		15.966	M1	3.32(6)	
	3d ⁵ [21]_5/2	3d ⁵ [34]_7/2		16.173	M1	1.27(6)	
	3d ⁵ [14]_9/2	3d ⁵ [29]_7/2		16.277	M1	2.61(6)	
	3d ⁵ [3]_7/2	3d ⁵ [18]_5/2		16.391	M1	1.29(6)	
	3d ⁵ [15]_1/2	3d ⁵ [30]_3/2		16.627	M1	2.72(6)	
	3d ⁵ [30]_3/2	3d ⁵ [37]_5/2		16.630	M1	2.79(6)	
	3d ⁵ [6]_9/2	3d ⁵ [19]_9/2		16.816	M1	2.56(6)	
	3d ⁵ [16]_3/2	3d ⁵ [30]_3/2		16.822	M1	3.84(6)	
	3d ⁵ [19]_9/2	3d ⁵ [32]_9/2		16.967	M1	2.17(6)	
	3d ⁵ [4]_3/2	3d ⁵ [16]_3/2		17.129	M1	3.32(6)	
	3d ⁵ [22]_3/2	3d ⁵ [33]_5/2		17.167	M1	1.30(6)	
	3d ⁵ [18]_5/2	3d ⁵ [30]_3/2		17.189	M1	1.14(6)	
	3d ⁵ [1]_5/2	3d ⁵ [4]_3/2	17.215	17.247	M1	3.76(6)	3.75(6) ^d
	3d ⁵ [4]_3/2	3d ⁵ [15]_1/2		17.336	M1	3.15(6)	
	3d ⁵ [1]_5/2	3d ⁵ [3]_7/2	17.660	17.660	M1	1.60(6)	1.59(6) ^d
	3d ⁵ [9]_7/2	3d ⁵ [21]_5/2		17.701	M1	1.52(6)	
	3d ⁵ [12]_7/2	3d ⁵ [28]_5/2		17.830	M1	1.71(6)	
	3d ⁵ [18]_5/2	3d ⁵ [29]_7/2		17.960	M1	1.21(6)	
	3d ⁵ [2]_5/2	3d ⁵ [11]_5/2		17.992	M1	6.55(6)	
	3d ⁵ [3]_7/2	3d ⁵ [14]_9/2		18.098	M1	1.42(6)	
	3d ⁵ [3]_7/2	3d ⁵ [12]_7/2		18.810	M1	1.42(6)	
	3d ⁵ [27]_5/2	3d ⁵ [36]_3/2		18.935	M1	1.39(6)	
	3d ⁵ [5]_11/2	3d ⁵ [13]_11/2	18.996	19.064	M1	2.31(6)	2.31(6) ^d
	3d ⁵ [7]_5/2	3d ⁵ [18]_5/2		19.102	M1	1.41(6)	
	3d ⁵ [7]_5/2	3d ⁵ [16]_3/2		19.577	M1	1.21(6)	
	3d ⁵ [8]_1/2	3d ⁵ [15]_1/2		21.017	M1	1.50(6)	
	3d ⁵ [1]_5/2	3d ⁵ [2]_5/2	21.203	21.317	M1	3.40(6)	3.40(6) ^d
W ⁵²⁺	3d ⁴ [22]_1	3d ⁴ [34]_0		11.156	M1	4.14(6)	
	3d ⁴ [7]_2	3d ⁴ [28]_1		11.369	M1	1.01(6)	
	3d ⁴ [10]_5	3d ⁴ [30]_4		12.299	M1	1.55(6)	

Table 2. (Continued.)

Ion	Lower level ^a	Upper level ^a	$\lambda_{\text{exp}}^{\text{b}}$ (nm)	$\lambda_{\text{MCDF}}^{\text{c}}$ (nm)	Type	$A_{\text{MCDF}}^{\text{c}}$ (s ⁻¹)	A_{prev} (s ⁻¹)
	3d ⁴ [13] ₃	3d ⁴ [30] ₄		13.401	M1	1.26(6)	
	3d ⁴ [5] ₃	3d ⁴ [17] ₄	13.543	13.513	M1	1.08(6)	1.09(6) ^d
	3d ⁴ [21] ₃	3d ⁴ [33] ₂		13.597	M1	2.49(6)	
	3d ⁴ [11] ₁	3d ⁴ [27] ₀		14.076	M1	3.39(6)	
	3d ⁴ [9] ₃	3d ⁴ [25] ₂		14.309	M1	1.71(6)	
	3d ⁴ [22] ₁	3d ⁴ [33] ₂		14.403	M1	3.62(6)	
	3d ⁴ [5] ₃	3d ⁴ [16] ₂		14.440	M1	3.16(6)	
	3d ⁴ [28] ₁	3d ⁴ [34] ₀		14.788	M1	8.45(6)	
	3d ⁴ [6] ₀	3d ⁴ [22] ₁		15.028	M1	3.62(6)	
	3d ⁴ [16] ₂	3d ⁴ [31] ₂		15.114	M1	1.81(6)	
	3d ⁴ [20] ₄	3d ⁴ [32] ₄		15.134	M1	5.00(6)	
	3d ⁴ [7] ₂	3d ⁴ [22] ₁		15.165	M1	4.00(6)	
	3d ⁴ [21] ₃	3d ⁴ [32] ₄		15.380	M1	3.20(6)	
	3d ⁴ [3] ₄	3d ⁴ [13] ₃		15.952	M1	1.75(6)	
	3d ⁴ [16] ₂	3d ⁴ [28] ₁		15.971	M1	1.71(6)	
	3d ⁴ [16] ₂	3d ⁴ [29] ₃		16.064	M1	1.25(6)	
	3d ⁴ [25] ₂	3d ⁴ [33] ₂		16.169	M1	2.74(6)	
	3d ⁴ [7] ₂	3d ⁴ [21] ₃		16.174	M1	4.51(6)	
	3d ⁴ [13] ₃	3d ⁴ [26] ₃		16.189	M1	1.81(6)	
	3d ⁴ [10] ₅	3d ⁴ [24] ₆		16.482	M1	1.75(6)	
	3d ⁴ [10] ₅	3d ⁴ [23] ₅		16.647	M1	1.07(6)	
	3d ⁴ [13] ₃	3d ⁴ [25] ₂		16.655	M1	1.85(6)	
	3d ⁴ [23] ₅	3d ⁴ [32] ₄		16.675	M1	1.27(6)	
	3d ⁴ [2] ₁	3d ⁴ [7] ₂	16.890	16.903	M1	4.71(6)	4.70(6) ^d
	3d ⁴ [8] ₄	3d ⁴ [20] ₄		17.006	M1	5.07(6)	
	3d ⁴ [2] ₁	3d ⁴ [6] ₀		17.076	M1	8.14(6)	
	3d ⁴ [12] ₆	3d ⁴ [24] ₆		17.171	M1	1.53(6)	
	3d ⁴ [15] ₂	3d ⁴ [25] ₂		17.174	M1	1.58(6)	
	3d ⁴ [9] ₃	3d ⁴ [21] ₃		17.186	M1	2.84(6)	
	3d ⁴ [17] ₄	3d ⁴ [30] ₄		17.238	M1	1.20(6)	
	3d ⁴ [4] ₂	3d ⁴ [11] ₁		17.377	M1	3.27(6)	
	3d ⁴ [17] ₄	3d ⁴ [29] ₃		17.391	M1	1.87(6)	
	3d ⁴ [9] ₃	3d ⁴ [20] ₄		17.505	M1	1.62(6)	
	3d ⁴ [3] ₄	3d ⁴ [10] ₅	17.846	17.855	M1	1.65(6)	1.65(6) ^d
	3d ⁴ [11] ₁	3d ⁴ [22] ₁		18.126	M1	1.83(6)	
	3d ⁴ [14] ₄	3d ⁴ [23] ₅		18.844	M1	1.40(6)	
	3d ⁴ [1] ₀	3d ⁴ [2] ₁	19.319	19.379	M1	3.32(6)	3.31(6) ^d
	3d ⁴ [3] ₄	3d ⁴ [8] ₄	19.445	19.543	M1	3.02(6)	3.02(6) ^d
	3d ⁴ [4] ₂	3d ⁴ [9] ₃		19.836	M1	1.37(6)	
	3d ⁴ [18] ₂	3d ⁴ [28] ₁		20.967	M1	1.12(6)	
	3d ⁴ [5] ₃	3d ⁴ [9] ₃		21.034	M1	1.92(6)	
W ⁵³⁺	3d ³ [8] _{7/2}	3d ³ [19] _{5/2}		12.036	M1	1.37(6)	
	3d ³ [1] _{3/2}	3d ³ [7] _{5/2}	12.312	12.282	M1	2.70(5)	2.75(5) ^d
	3d ³ [10] _{3/2}	3d ³ [19] _{5/2}		13.303	M1	2.66(6)	
	3d ³ [12] _{5/2}	3d ³ [19] _{5/2}		14.027	M1	2.02(6)	
	3d ³ [4] _{7/2}	3d ³ [14] _{5/2}		14.190	M1	1.09(6)	
	3d ³ [2] _{5/2}	3d ³ [10] _{3/2}		14.749	M1	1.98(6)	
	3d ³ [10] _{3/2}	3d ³ [18] _{3/2}		14.907	M1	2.74(6)	
	3d ³ [7] _{5/2}	3d ³ [16] _{3/2}		14.991	M1	2.39(6)	
	3d ³ [3] _{3/2}	3d ³ [12] _{5/2}		15.036	M1	2.46(6)	
	3d ³ [11] _{1/2}	3d ³ [18] _{3/2}		15.467	M1	1.81(6)	
	3d ³ [14] _{5/2}	3d ³ [19] _{5/2}		15.588	M1	1.60(6)	
	3d ³ [8] _{7/2}	3d ³ [17] _{9/2}		15.730	M1	3.98(6)	
	3d ³ [6] _{9/2}	3d ³ [13] _{11/2}	15.785	15.792	M1	1.42(6)	1.42(6) ^d
	3d ³ [12] _{5/2}	3d ³ [18] _{3/2}		15.822	M1	2.54(6)	
	3d ³ [3] _{3/2}	3d ³ [10] _{3/2}		15.968	M1	4.33(6)	
	3d ³ [1] _{3/2}	3d ³ [5] _{1/2}	16.027	16.035	M1	1.03(6)	1.02(6) ^d
	3d ³ [5] _{1/2}	3d ³ [11] _{1/2}		16.478	M1	4.37(6)	
	3d ³ [2] _{5/2}	3d ³ [8] _{7/2}		16.696	M1	4.89(6)	
	3d ³ [9] _{9/2}	3d ³ [17] _{9/2}		16.746	M1	2.87(6)	

Table 2. Continued.

Ion	Lower level ^a	Upper level ^a	$\lambda_{\text{exp}}^{\text{b}}$ (nm)	$\lambda_{\text{MCDF}}^{\text{c}}$ (nm)	Type	$A_{\text{MCDF}}^{\text{c}}$ (s ⁻¹)	A_{prev} (s ⁻¹)
W ⁵⁴⁺	3d ³ [1] _{3/2}	3d ³ [3] _{3/2}	17.216	17.243	M1	2.76(6)	2.74(6) ^d
	3d ³ [4] _{7/2}	3d ³ [9] _{9/2}		18.051	M1	1.30(6)	
	3d ³ [6] _{9/2}	3d ³ [9] _{9/2}		18.061	M1	2.28(6)	
	3d ³ [1] _{3/2}	3d ³ [2] _{5/2}	18.867	18.933	M1	3.42(6)	3.41(6) ^d
	3d ³ [4] _{7/2}	3d ³ [8] _{7/2}		19.402	M1	1.19(6)	
	3d ³ [7] _{5/2}	3d ³ [14] _{5/2}		19.911	M1	1.17(6)	
	3d ² [5] ₁	3d ² [9] ₀		12.757	M1	7.83(6)	
	3d ² [1] ₂	3d ² [4] ₂	14.959	14.980	M1	1.81(6)	1.81(6) ^d
							1.798(6) ^e
	3d ² [3] ₃	3d ² [7] ₄		15.369	M1	3.82(6)	
W ⁵⁵⁺	3d ² [4] ₂	3d ² [8] ₂		15.848	M1	3.11(6)	
	3d ² [5] ₁	3d ² [8] ₂		16.907	M1	1.30(6)	
	3d ² [1] ₂	3d ² [3] ₃	17.080	17.138	M1	3.68(6)	3.683(6) ^e
	3d ² [6] ₄	3d ² [7] ₄		18.621	M1	1.09(6)	
	3d ² [2] ₀	3d ² [5] ₁	19.177	19.222	M1	1.74(6)	1.72(6) ^d
							1.771(6) ^e
	3d[1] _{3/2}	3d[2] _{5/2}	15.962	16.008	M1	2.59(6)	2.59(6) ^d
							1.48(6) ^f
W ⁵⁷⁺	3p ⁵ [1] _{3/2}	3p ⁵ [2] _{1/2}		3.563	M1+E2	3.95(8)	3.91(8) ^g
	3p ⁴ [3] ₁	3p ⁴ [5] ₀		3.402	M1	8.43(8)	
	3p ⁴ [1] ₂	3p ⁴ [4] ₂		3.473	M1+E2	2.09(8)	2.14(8) ^h
	3p ⁴ [4] ₂	3p ⁴ [5] ₀		3.495	E2	2.36(7)	
	3p ⁴ [1] ₂	3p ⁴ [3] ₁		3.570	M1+E2	3.33(8)	3.42(8) ^h
	3p ⁴ [2] ₀	3p ⁴ [4] ₂		3.679	E2	1.69(6)	1.86(6) ^h
	3p ⁴ [2] ₀	3p ⁴ [3] ₁		3.788	M1	1.14(8)	1.18(8) ^h
	3p ³ [2] _{3/2}	3p ³ [5] _{3/2}		3.344	M1+E2	4.43(8)	4.40(8) ⁱ
	3p ³ [1] _{3/2}	3p ³ [4] _{1/2}		3.360	M1+E2	2.28(8)	2.24(8) ⁱ
	3p ³ [3] _{3/2}	3p ³ [5] _{3/2}		3.455	M1+E2	1.20(8)	1.19(8) ⁱ
W ⁵⁹⁺	3p ³ [1] _{3/2}	3p ³ [3] _{5/2}		3.508	M1+E2	7.30(7)	7.24(7) ⁱ
	3p ³ [4] _{1/2}	3p ³ [5] _{3/2}		3.612	M1+E2	9.74(7)	9.72(7) ⁱ
	3p ³ [1] _{3/2}	3p ³ [2] _{3/2}		3.631	M1+E2	3.84(8)	3.73(8) ⁱ
	3p ² [2] ₁	3p ² [5] ₀		3.218	M1	4.84(8)	4.80(8) ^j
	3p ² [3] ₂	3p ² [5] ₀		3.299	E2	1.59(7)	1.49(7) ^j
	3p ² [2] ₁	3p ² [4] ₂		3.401	M1+E2	2.17(8)	2.16(8) ^j
	3p ² [1] ₀	3p ² [3] ₂		3.469	E2	4.58(6)	4.61(6) ^j
	3p ² [3] ₂	3p ² [4] ₂		3.492	M1+E2	2.17(8)	2.15(8) ^j
	3p ² [1] ₀	3p ² [2] ₁		3.563	M1	2.65(8)	2.61(8) ^j
	3p[1] _{1/2}	3p[2] _{3/2}		3.408	M1+E2	2.25(8)	2.24(8) ^k
W ⁶¹⁺							2.13(8) ^l

^aLevel designations from table 1. ^bFrom Ralchenko *et al* (2011a). ^cThis work. ^dFAC calculations from Ralchenko *et al* (2011a). ^eRMBPT calculations from Safronova & Safronova (2010). ^fRQDO calculations from Charro *et al* (2002). ^gMCDF calculations from Huang *et al* (1983). ^hMCDF calculations from Saloman and Kim (1989). ⁱMCDF calculations from Huang (1984). ^jMCDF calculations from Huang (1985). ^kMCDF calculations from Huang (1986). ^lRQDO calculations from Charro *et al* (2003).

3p to 4p and to 4f orbitals were considered by including the following configurations: $3s^23p^k + 3p^{k+2} + 3s3p^k3d + 3s^23p^{k-2}3d^2 + 3p^k3d^2 + 3s^23p^{k-1}4p + 3s^23p^{k-1}4f$. Similarly, for the 3d^k configurations (ions W⁴⁷⁺ through W⁵⁵⁺), all single and double excitations within the $n = 3$ complex together with the single excitations from 3d to 4s and 4d orbitals were included by considering the following multiconfiguration expansions: $3s^23p^63d^k + 3s^23p^43d^{k+2} + 3s3p^63d^{k+1} + 3p^63d^{k+2} + 3s^23p^63d^{k-1}4s + 3s^23p^63d^{k-1}4d$.

The calculations were completed with the inclusion of the relativistic two-body Breit interaction and of the quantum

electrodynamic corrections due to self-energy and vacuum polarization using the routines developed by McKenzie *et al* (1980). In these routines, the leading corrections to the Coulomb repulsion between electrons in quantum electrodynamics are considered as a first-order perturbation using the transverse Breit operator given by Grant and McKenzie (1980), the second-order vacuum polarization corrections are evaluated using the prescription of Fullerton and Rinker (1976), and the self-energy contributions are estimated by interpolating the values obtained by Mohr (1974, 1975) for 1s, 2s and 2p Coulomb orbitals. For each ion,

the nuclear effects were estimated by considering a uniform charge distribution with the usual atomic weight of tungsten, i.e. 183.85.

3. Results and discussion

3.1. Energy levels

The energy level values obtained using the MCDF method described above for the $3p^k$ and $3d^k$ ground configurations of tungsten ions from W^{47+} to W^{61+} are presented in table 1. The leading compositions of the computed eigenvectors in the jj -coupling scheme are also given in that table. In the notations adopted, nl_- corresponds to the case $j_- = l-1/2$, while nl is written for $j_+ = l+1/2$. As expected for such highly ionized atoms, it was verified that this coupling appears much more adequate than the LS one. Indeed, the average jj purities obtained in this work were found to be equal to 99% and 88%, for $3p^k$ and $3d^k$ configurations, respectively, while the corresponding average LS contributions were found to range from 77% to 52%. Consequently, the jj designation has been used throughout this paper. For simplicity, in table 1 each energy level belonging to a particular ion is labelled as $nl^k[i]_J$ where nl^k is the electronic configuration, i is an order number in this configuration and J is the total angular momentum.

Ab initio theoretical energies computed in this work are also compared in table 1 with available values taken from the latest NIST compilation (Ralchenko *et al* 2011b). For $3p^k$ and $3d^k$ ground configurations of tungsten ions, the energy levels reported in this compilation were taken from the recent paper due to Kramida (2011) who significantly updated and extended the spectroscopic data of highly ionized tungsten previously published by Kramida and Shirai (2009). In particular, the observations of Ralchenko *et al* (2011a) were used to deduce new experimental energy levels in $3d^k$ ground configurations of tungsten ions. When comparing our MCDF results with these experimental values, a very good agreement is observed, the relative difference remaining below 0.5%. We also note an excellent agreement between our computed energies and those of Kramida (2011) obtained by theoretical calculation from the work of Ralchenko *et al* (2011a) or determined by interpolation or extrapolation of known experimental values. Some other energies, not reported in table 1 neither in the latest NIST compilation, were computed by Kramida and Shirai (2009) using Cowan's code (Cowan 1981). Even if the general agreement between those values and our results is rather good, larger discrepancies (up to 15%) can be observed. However, it is expected that, for highly charged ions such as those considered here, the fully relativistic MCDF approach used in this work is more appropriate, and consequently more accurate, than the pseudo-relativistic Hartree–Fock approximation used by Kramida and Shirai (2009).

3.2. Wavelengths and transition probabilities

The MCDF method described above was used for calculating wavelengths and transition probabilities for magnetic dipole (M1) and electric quadrupole (E2) radiations corresponding to the transitions between all energy levels within the $3p^k$ and

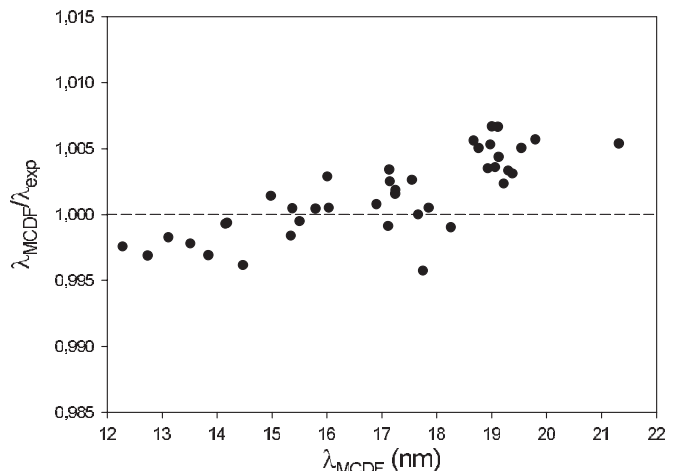


Figure 1. Comparison between calculated wavelengths (λ_{MCDF}) as obtained in this work and experimental values published by Ralchenko *et al* (2011a) for magnetic dipole (M1) lines within $3d^k$ ground configurations of tungsten ions from W^{47+} to W^{55+} .

$3d^k$ ground configurations of highly charged tungsten ions. Our results are listed in table 2. If the two types of radiation contribute significantly to the total intensity of a line, the sum of both A -values is given. The exclusion criterion of one particular type of radiation for a given transition is that the corresponding transition probability should be less than 1% of the sum of M1 and E2 contributions. Owing to the extensive nature of the results, only transitions for which A is greater than 10^6 s $^{-1}$ are reported in the table if we except a few weaker lines observed experimentally. It is worth mentioning that, while M1 contributions were found to dominate by far E2 ones in the $3d^k$ configurations, both types of radiation appear for forbidden lines within the $3p^k$ configurations.

Our calculated wavelengths are also compared with the available experimental values in table 2. These experimental values were obtained by Ralchenko *et al* (2008, 2011a) who observed a total of 40 M1 transitions in tungsten ions from W^{47+} to W^{55+} from extreme ultraviolet EBIT spectra between 10 and 25 nm. In most cases, the present results agree very well with the measured wavelengths, the mean ratio $\lambda_{MCDF}/\lambda_{exp}$ being found equal to 1.001 ± 0.003 , as illustrated in figure 1 showing this ratio as a function of λ_{MCDF} . For these ions, Ralchenko *et al* (2011a) also reported transition probabilities computed using the relativistic FAC developed by Gu (2007). As seen in table 2, their results are in excellent agreement with A -values calculated in this work. We also note that the RMBPT calculations published by Safranova and Safranova (2010) for W^{54+} ion agree with our transition probabilities to within 2%, while the RQDO calculations of Charro *et al* (2002) give a transition probability for the $3d[1]_{3/2}-3d[2]_{5/2}$ transition in W^{55+} a factor of about 2 smaller than the one obtained in our work. However, for this particular line, our A -value is in excellent agreement with the recent calculation of Ralchenko *et al* (2011a) which implies that the result published by Charro *et al* is probably less accurate. For tungsten ions with an open $3p$ shell (W^{57+} through W^{61+}), previous MCDF calculations due to Huang *et al* (1983), Saloman and Kim (1989) and Huang (1984, 1985, 1986)

are also reported in table 2. Although obtained by using slightly smaller multiconfiguration expansions, these latter results agree very well (within a few per cent) with transition probabilities computed in this work.

4. Conclusion

Using the fully relativistic multiconfiguration Dirac–Fock method, a new set of theoretical wavelengths and transition probabilities has been obtained for forbidden lines within the $3p^k$ and $3d^k$ ground configurations of highly charged tungsten ions from W^{47+} to W^{61+} . These lines appear in the x-ray spectral range from 3 to 4 nm and the extreme ultraviolet region from 11 to 23 nm for $3p^k$ and $3d^k$ ions, respectively. The new results reported in this work considerably increase the number of data available for forbidden lines in tungsten ions. They are expected to be useful for plasma diagnostics and modelling in fusion reactors.

Acknowledgment

The author is Senior Research Associate of the Belgian FRS-FNRS. Financial support from this organization is acknowledged.

References

- Charro E, Curiel Z and Martin I 2002 *Astron. Astrophys.* **387** 1146
 Charro E, Lopez-Ferrero S and Martin I 2003 *Astron. Astrophys.* **406** 741
 Clementson J, Beiersdorfer P and Gu M F 2010 *Phys. Rev. A* **81** 012505
 Cowan R D 1981 *The Theory of Atomic Structure and Spectra* (Berkeley, CA: University of California Press)
 Ding X B *et al* 2011 *J. Phys. B : At. Mol. Opt. Phys.* **44** 145004
 Doron R and Feldman U 2001 *Phys. Scr.* **64** 319
 Dyall K G, Grant I P, Johnson C T, Parpia F A and Plummer E P 1989 *Comput. Phys. Commun.* **55** 425
 Feldman U, Doron R, Klapisch M and Bar-Shalom A 2001 *Phys. Scr.* **63** 284
 Feldman U, Indelicato P and Sugar J 1991 *J. Opt. Soc. Am. B* **8** 3
 Fullerton L W and Rinker G A 1976 *Phys. Rev. A* **13** 1283
 Grant I P and McKenzie B J 1980 *J. Phys. B: At. Mol. Phys.* **13** 2671
 Gu M F 2007 *Can. J. Phys.* **86** 675
 Hawryluk R J *et al* 2009 *Nucl. Fusion* **49** 065012
 Huang K N 1984 *At. Data Nucl. Data Tables* **30** 313
 Huang K N 1985 *At. Data Nucl. Data Tables* **32** 503
 Huang K N 1986 *At. Data Nucl. Data Tables* **34** 1
 Huang K N, Kim Y K, Cheng K T and Desclaux J P 1983 *At. Data Nucl. Data Tables* **28** 355
 Jonauskas V, Kisielius R, Kyniene A, Kucas S and Norrington P H 2010 *Phys. Rev. A* **81** 012506
 Kramida A E 2011 *Can. J. Phys.* **89** 551
 Kramida A E and Shirai T 2009 *At. Data Nucl. Data Tables* **95** 305
 McKenzie B J, Grant I P and Norrington P H 1980 *Comput. Phys. Commun.* **21** 233
 Mohr P J 1974 *Ann. Phys.* **88** 52
 Mohr P J 1975 *Phys. Rev. Lett.* **34** 1050
 Neu R, Fournier K B, Bolshukhin D and Dux R 2001 *Phys. Scr. T* **92** 307
 Neu R, Fournier K B, Schlägl D and Rice J 1997 *J. Phys. B : At. Mol. Opt. Phys.* **30** 5057
 Norrington P H 2009 <http://www.am.qub.ac.uk/DARC/>
 Porto J V, Kink I and Gillaspy J D 2000 *Phys. Rev. A* **61** 054501
 Pospieszczyk A 2006 *Nuclear Fusion Research* (Berlin: Springer)
 Pütterich T, Neu R, Biedermann C and Radtke R (ASDEX Upgrade Team) 2005 *J. Phys. B : At. Mol. Opt. Phys.* **38** 2071
 Quinet P, Vinogradoff V, Palmeri P and Biémont E 2010 *J. Phys. B : At. Mol. Opt. Phys.* **43** 144003
 Radtke R, Biedermann C, Fussmann G, Schwob J L, Mandelbaum P and Doron R 2007 *Atomic and Plasma-Material Interaction Data for Fusion* vol 13 (Vienna: International Atomic Energy Agency)
 Ralchenko Yu, Draganic I N, Osin D, Gillaspy J D and Reader J 2011a *Phys. Rev. A* **83** 032517
 Ralchenko Yu, Draganic I N, Tan J N, Gillaspy J D, Pomeroy J M, Reader J, Feldman U and Holland G E 2008 *J. Phys. B : At. Mol. Opt. Phys.* **41** 021003
 Ralchenko Yu, Kramida A E and Reader J (NIST ASD Team) 2011b *NIST Atomic Spectra Database* v.4.1.0
 Ralchenko Yu, Reader J, Pomeroy J M, Tan J N and Gillaspy J D 2007 *J. Phys. B : At. Mol. Opt. Phys.* **40** 3861
 Ralchenko Yu, Tan J N, Gillaspy J D, Pomeroy J M and Silver E 2006 *Phys. Rev. A* **74** 042514
 Safranova U I and Safranova A S 2010 *J. Phys. B : At. Mol. Opt. Phys.* **43** 074026
 Saloman E B and Kim Y K 1989 *At. Data Nucl. Data Tables* **41** 339
 Tragin N, Geindre J-P, Monier P, Gauthier J-C, Chenais-Popovics C, Wyart J-C and Bauche-Arnoult C 1988 *Phys. Scr.* **37** 72
 Utter S B, Beiersdorfer P and Brown G V 2000 *Phys. Rev. A* **61** 030503